Sensitivity analysis for the tolerancing of gear profiles with stochastic errors

M. Rajabalinejad
Delft University of Technology, Delft, the Netherlands

Abstract:
This paper introduces the concept of the 'sensitivity chart' as an applied tool to evaluate the effect of profile modifications on the load factor of gears with stochastic indexing errors and to find optimal solutions. The embedded ability to evaluate different solutions simultaneously also allows the analysis of the sensitivity of technical designs to variations in the manufacturing parameters, from which the term 'sensitivity chart' is derived. To build a sensitivity chart, the exact geometry of tooth meshing is incorporated into a dynamical non-linear model of the considered gear system, seamlessly embedding the effect of pitch errors, tooth separation, degree-of-freedom coupling, and profile modifications. Various possible combinations of error distributions and profile corrections are applied to the gear model, which is simulated dynamically to calculate the load factor. The sensitivity charts are compiled by post-processing and interpolation of this simulation data.

Keywords: gear vibration, indexing errors, profile modifications, dynamic load factor, dynamical simulation, sensitivity chart

1. INTRODUCTION

Gears with indexing errors are known to undergo impact loading ranging from mild to quite severe, depending on the extent and distribution of the errors. The most unfavourable scenario is the linear (saw-tooth) distribution of indexing errors, which is the result of the accumulation of small consecutive indexing errors in conventional or CNC machine tools when there is either a mismatch between the linear motion of the machine bed and the indexing rotation of the work-piece chuck [1] or due to deflections from the cutting forces.

While strengthening the tooth profile by various means is a design possibility on which much research also exists [2-14], the established remedy to lessen the impacts and overloads caused by indexing errors is by applying modifications on the tooth profiles. Tip relief, root relief, or a combination of both, are all accepted ways of modification, with tip relief being the simplest and most popular [15]. The selection and dimensioning of these profile modifications, also termed 'corrections' has been documented in various guidelines and standards as in AGMA [16-17], Maag [18], Dudley [19], and Niemann and Winter [20], but have not been studies as thoroughly as the corresponding solutions for tooth strength cited previously. These guidelines consider the statically loaded gear pair and introduce a profile modification equal to the maximum indexing error. In vibration-critical applications the calculated profile modification is increased to anticipate the cumulative effect of elastic deflections due to tooth bending. These deflections are normally calculated from statical analysis [15], however more accurate predictions can be made by dynamical simulation.

The objective of these modifications is to eliminate the possibility of detrimental tip contact during tooth engagement, which is affected by material removal. It should be noted that these corrections are, strictly speaking, errors in themselves and that their introduction is clearly a compromise. In fact, it has been observed that excessive corrections can lead to increased transmission errors (TE), deterioration of the vibratory response and to even worse overloads. Thus arise the questions: How sensitive are gears with indexing errors to the selection of profile modification? Are there tolerance limits? How much precision is needed in applying a modification on a given gear of given precision? Standards and guidelines so far do not provide such a sensitivity analysis, leaving the

optimal selection for any particular application to experience and trial-and-error, which can be tedious and costly.
In this paper a methodology is proposed for conducting this sensitivity analysis, using 'sensitivity charts' derived from dynamical simulation. Common linear single-DOF models are not detailed enough and coupled multi-DOF models either consider an abstracted gear mesh geometry, or are not built to take into account combined indexing errors and profile modifications. On the other hand, accurate geometrical models such as in Litvin [21] have still not made the transition from quasi-statical to truly dynamical analysis [22], so their results can only be indicative of what might be expected under real dynamic conditions.

In this paper the mesh analysis models by Spitas et al. [23-25] are used, allowing detailed calculation of the operating transmission errors as a function of the actual tooth form, including corrections. No simplifying assumptions are made in developing this theory and it is possible to model individual errors and complex error distributions. The mesh analysis results are then fed into a detailed dynamical model comprising 3 DOFs/ gear, which takes into account torsional-bending vibration coupling, friction and tooth separation. Tooth interference is calculated individually for each pair in real time to avoid simplifying assumptions and achieve realistic modelling of the dynamical response of gears with errors.
This model is used to simulate the dynamical response of a single-stage spur gear speed reducer and a range of combinations of indexing error distributions and corrective profile modifications is considered. These results are used to predict the lateral force amplitude and dynamic load factor in each case, which are used as performance indices. Sensitivity charts are then plotted from these results, which help identify the optimal corrections, tolerance limits and precision requirements for given gear designs. Various examples on the use of these sensitivity charts are presented to demonstrate their application.

2. NOMENCLATURE

symbol	definition	symbol	definition
θ_i	angular position of gear i (additional subscripts: n, ref defined in the text)	k_k	instant stiffness of individual tooth pair k
$\mathbf{s}_i$	deflection vector of DOF i	c_{hyst}	damping coefficient due to tooth material hysterisis
θ_s	slip angle	f_k	instant friction coefficient of individual tooth pair k
δ_k	angular interference of tooth pair k		
		$\mathbf{F}_{k,elast}$	elastic component of the contact force of tooth pair k
i_{12}	transmission ratio	$\mathbf{F}_{k,hyst}$	hysteretic component of the contact force of tooth pair k
I_{12}	directional index (equal to 1 for external gears, -1 for internal gears)	$\mathbf{F}_{k,frict}$	frictional component of the contact force of tooth pair k
$\mathbf{r}_i$, $\mathbf{r}_{i,k}$	position vector of a contact point in relation to centre of gear i (the optional k index refers to a specific tooth pair)		
$\mathbf{f}_i$	vector function of tooth profile of gear i	$\mathbf{M}_i$	mass matrix of rotating element i
$\mathbf{a}_{12}$	centre distance vector	$\mathbf{C}_i$	damping coefficient for bending of shaft i due to hysterisis
$\mathbf{R}$	generic rotary translation matrix	$\mathbf{K}_i$	lumped bending stiffness matrix of DOF i (shaft with elastic supports: bearings/ housing)
$\hat{\mathbf{x}}_i$	unitary vector along the x_i direction, where i=1,2,3 (in Cartesian coordinates)	J_i	mass moment of inertia of rotating element i

$\mathbf{n}_k$	normal unitary vector at contact point of tooth pair k	D_i	damping coefficient related to rotation of DOF i (i.e. windage)
$\mathbf{m}_k$	unitary vector along the direction of instant sliding velocity of tooth pair k	E_{i-j}	damping coefficient for torsion of shaft segment i-j due to hysterisis
$\sigma^{(j)}$, σ_o, σ_{or}	anticipated indexing error of tooth j, maximum anticipated indexing error, maximum real indexing error	G_{i-j}	torsional stiffness of shaft segment i-j
$U\sigma, L\sigma$	upper and lower tolerance for the maximum indexing error σ_o		
m, m_r	prescribed modification (equal to maximum slip angle θ_s), actual modification		
Um, Lm	upper and lower tolerance for the modification m		

3. MODELLING OF GEAR MESHING GEOMETRY

3.1. Formulation of the meshing equations

Let us assume a pair of gears and their respective teeth 1 and 2 in contact as shown in Fig. 1. If tooth 1 is regarded as the reference and conjugate gear action is assumed, then tooth 2 should be at a nominal angular position θ_{2n}, such that:

$$\theta_1 - \theta_{1ref} = -I_{12} i_{12} (\theta_{2n} - \theta_{2ref}) \tag{1}$$

where θ_{1ref} and θ_{2ref} are tooth reference positions.

In fact, no conjugacy requirement will be made in this analysis, so the actual position θ_2 of tooth 2 will deviate from the nominal θ_{2n} by an angle θ_s, which expresses the relative slip of the operating pitch circles of both gears (slip angle).

$$\theta_2 - \theta_{2n} = \theta_s \tag{2}$$

The working part of each tooth profile is assumed to be a C^1 continuous curve, so any contact point A should simultaneously satisfy the following two equations:

$$\mathbf{r}_1 - \mathbf{r}_2 = \mathbf{a}_{12} \tag{3}$$

$$\frac{\partial \mathbf{r}_1}{\partial r_1} \times \frac{\partial \mathbf{r}_2}{\partial r_2} = \mathbf{0} \tag{4}$$

where $\mathbf{r}_1 = \overrightarrow{O_1 A}$ and $\mathbf{r}_2 = \overrightarrow{O_2 A}$ in the global coordinate system.

At this point the generic rotary translation matrix is introduced:

$$\mathbf{R}_j = \begin{bmatrix} \cos\theta_j & -\sin\theta_j & 0 \\ \sin\theta_j & \cos\theta_j & 0 \\ 0 & 0 & 1 \end{bmatrix} \tag{5}$$

where θ_j is any arbitrary rotation angle about the axis of rotation of the gear. If the profile of a tooth of gear 1 at an arbitrary reference position $\theta_1 = 0$ is described by a parametric vector function $\mathbf{f}_1$, then the following equations are true:

$$\mathbf{r}_1 = \mathbf{f}_1 \tag{6}$$

$$r_1 = \|\mathbf{f}_1\| \tag{7}$$

where r_1 serves as the profile function parameter and the operator $\|\cdot\|$ denotes the Euclidian norm. The same tooth profile at any other rotation angle can be expressed as:

$$\mathbf{r}_1 = \mathbf{R}_1 \mathbf{f}_1 \tag{8}$$

Similar definitions apply to the teeth of gear 2. In this case r_2 is the profile function parameter so that in general:

$$\mathbf{r}_2 = \mathbf{R}_2\mathbf{f}_2 \tag{9}$$

Introducing the slip angle θ_s and considering Eqs. (2, 5) it is easy to derive the following expression:

$$\mathbf{R}_2 = \mathbf{R}_{2n}\mathbf{R}_s \tag{10}$$

so that Eq. (9) becomes:

$$\mathbf{r}_2 = \mathbf{R}_{2n}\mathbf{R}_s\mathbf{f}_2 \tag{11}$$

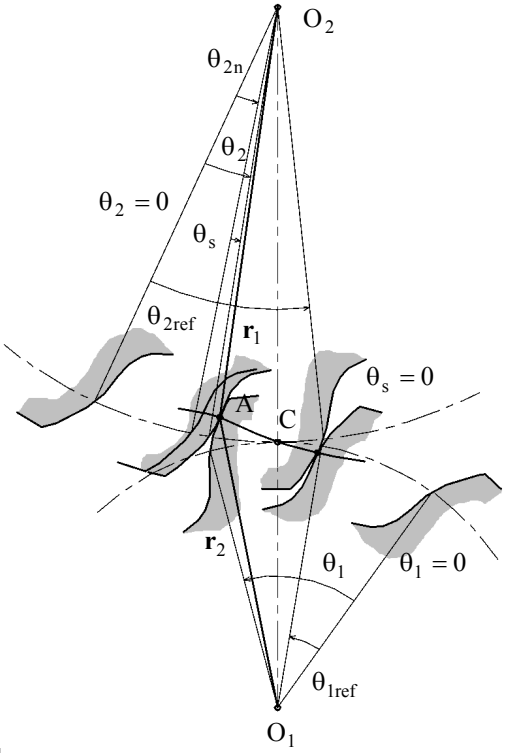

Fig. 1
Gear contact geometry

Finally, substituting Eqs. (8, 11) into Eqs. (3-4), it is possible to arrive at a different form of the equations of meshing as follows:

$$\mathbf{R}_1\mathbf{f}_1 - \mathbf{R}_{2n}\mathbf{R}_s\mathbf{f}_2 = \mathbf{a}_{12} \tag{12}$$

$$\mathbf{R}_1\frac{\partial\mathbf{f}_1}{\partial r_1}\times\mathbf{R}_{2n}\mathbf{R}_s\frac{\partial\mathbf{f}_2}{\partial r_2} = \mathbf{R}_1\frac{d\mathbf{f}_1}{dr_1}\times\mathbf{R}_{2n}\mathbf{R}_s\frac{d\mathbf{f}_2}{dr_2} = \mathbf{0} \tag{13}$$

These are the general equations that relate the positions of teeth 1, 2 to their shapes. Obviously, if the tooth shapes are known in the form of functions $\mathbf{f}_1$ and $\mathbf{f}_2$, then the path of contact and the TE, if any, can be uniquely calculated.

3.2. Solution of the meshing equations

Here the slip angle θ_s will be calculated as a function of the reference gear position θ_1 for known tooth profile functions $\mathbf{f}_1(r_1)$ and $\mathbf{f}_2(r_2)$.

By solving Eq. (12) in terms of r_2 we obtain:

$$r_2 = \left\|\mathbf{R}_1\mathbf{f}_1 - \mathbf{a}_{12}\right\| = U_1(\theta_1, r_1) \tag{14}$$

It can be observed (Fig. 1) that vectors $\mathbf{f}_2$ and $\mathbf{R}_2\mathbf{f}_2 = \mathbf{R}_{2n}\mathbf{R}_s\mathbf{f}_2$ form by default an angle equal to $\theta_2 = \theta_{2n} + \theta_s$, therefore:

$$\theta_2 = \pm\cos^{-1}\left\{\frac{\mathbf{R}_2\mathbf{f}_2\cdot\mathbf{f}_2}{\left\|\mathbf{R}_2\mathbf{f}_2\right\|\left\|\mathbf{f}_2\right\|}\right\}$$

$$\theta_{2n}+\theta_s=\pm\cos^{-1}\left\{\frac{[\mathbf{R}_1\mathbf{f}_1-\mathbf{a}_{12}]\cdot\mathbf{f}_2}{\|\mathbf{R}_1\mathbf{f}_1-\mathbf{a}_{12}\|\|\mathbf{f}_2\|}\right\}$$

Finally by inserting Eq. (14) we obtain:

$$\theta_s=-\theta_{2n}\pm\cos^{-1}\left\{\frac{1}{r_2^2}[\mathbf{R}_1\mathbf{f}_1-\mathbf{a}_{12}]\cdot\mathbf{f}_2\right\}=U_2(\theta_1,r_1,r_2) \tag{15}$$

Since vectors $\frac{d\mathbf{f}_1}{dr_1}$ and $\frac{d\mathbf{f}_2}{dr_2}$ lie on the same plane, which is normal to the axis of revolution, a scalar equivalent of Eq. (13) can be obtained:

$$\left(\mathbf{R}_1\frac{d\mathbf{f}_1}{dr_1}\times\mathbf{R}_{2n}\mathbf{R}_s\frac{d\mathbf{f}_2}{dr_2}\right)\cdot\hat{\mathbf{x}}_3=U_3(\theta_1,r_1,r_2,\theta_s)=0 \tag{16}$$

where $\hat{\mathbf{x}}_3$ is the unitary vector along the x_3-axis (axis of revolution).

Substituting Eqs. (14-15) into Eq. (16) we obtain a scalar equation involving r_1 only, with θ_1 being the independent parameter:

$$U_3(\theta_1,r_1,U_1(\theta_1,r_1),U_2(\theta_1,r_1,U_1(\theta_1,r_1)))=0 \tag{17}$$

Eq. (17) can be solved in terms of r_1 and subsequently Eqs. (14-15) can be solved explicitly in terms of r_2 and θ_s respectively, thus forming a parametric solution to the tooth meshing problem, with the reference gear position θ_1 as the independent parameter.

3.3. Implementation of pitch errors and profile corrections

Considering the above analysis, it is possible to obtain the appropriate function of θ_s for modified profiles or profiles with errors. From the meshing analysis standpoint, these two variants are treated in exactly the same way and profile modifications can be regarded as 'deliberate' errors. Implementing pitch errors and/ or profile corrections requires the input of the modified profile functions $\mathbf{f}_1$ and $\mathbf{f}_2$.

4. DYNAMICAL MODELLING

4.1. Contact forces

Gear teeth are subjected to a) elastic, b) internal friction (hysteretic) [26] and c) frictional contact forces and deform as cantilever beams of varying cross-section with elastic foundation [27]; local Hertzian contact pressure displacements are also taken into account [28]. The hysteretic friction component is negligible for the usual gear materials (i.e. steel), but it plays a role in assuring the stability of time-domain simulations of the dynamical response [29].

The force components at a given contact point, designated by index k, are calculated as functions of the interference δ_k from the Eq. (18-20). By default they are considered to act on the teeth of the reference gear (gear 1).

$$\mathbf{F}_{k,elast}=-|\delta_k|k_k\mathbf{n}_k \tag{18}$$

$$\mathbf{F}_{k,hyst}=c_{hyst}\frac{d|\delta_k|}{dt}\mathbf{n}_k \tag{19}$$

$$\mathbf{F}_{k,frict}=|\delta_k|f_k k_k\mathbf{m}_k \tag{20}$$

where $\mathbf{n}_k$ is the unitary normal vector to the tooth profile at the contact point (pointing outwards) and $\mathbf{m}_k$ is the unitary vector in the direction of the sliding velocity. By default it is $\mathbf{m}_k\perp\mathbf{n}_k$.

Eq. (19) represents the basic linear viscoelastic model (Voigt – Kelvin model) of the inelastic damping forces [30]. There is currently no general agreement regarding the calculation of the damping coefficients and usually the linear damping model is considered primarily for convenience [29]. The popular practice of estimating a fairly realistic constant value of ζ=0.1 for the non-

dimensional damping coefficient has been adopted [29]. The stiffness coefficient k_k is generally a function of tooth position and can be calculated from a) analytical/ empirical formulae [27-28], b) Finite/Boundary Element Analysis [31-32] or c) a hybrid method combining the first two [33]. Here the formulae of [27-28] were used. These offer good calculation speed and comparisons with Finite Element results have shown good correlation.

4.2. Gearbox model

The layout studied in this paper is shown in Fig. 2. The motor element (0) provides the power at a controlled speed through shaft I to gear 1 (DOF 1) and then, through the tooth mesh (III) to gear 2 (DOF 2). The power is then transmitted through shaft II to the break element (DOF 3), where a controlled torque is applied. The 'analysis plane' and its universal coordinate system are also defined, with axis x_3 being the axis of revolution.

The free DOFs are identified in Fig. 3. Spur gear shafts are seldom placed in cantilever arrangements, so bending of the shafts is not considered to affect the parallelism of gears (1) and (2) significantly and hence the rotations of the gear centres about the axes x_1 and x_2 and the corresponding DOFs can be neglected. This brings along the additional advantage of allowing each shaft- bearing system to be modelled as a lump element of combined stiffness.

With respect to the free DOFs the dynamical equations are as follows.

$$J_1 \frac{d^2}{dt^2}\theta_1 + D_1 \frac{d}{dt}\theta_1 - \hat{\mathbf{x}}_3 \cdot \sum_k \left[\mathbf{r}_{1,k} \times \left(\mathbf{F}_{k,elast} + \mathbf{F}_{k,hyst} + \mathbf{F}_{k,frict}\right)\right] - E_{0-1}\left(\frac{d}{dt}\theta_0 - \frac{d}{dt}\theta_1\right) - G_{0-1}(\theta_0 - \theta_1) = 0 \tag{21}$$

$$\mathbf{M}_1 \frac{d^2}{dt^2}\mathbf{s}_1 - \sum_k \left(\mathbf{F}_{k,elast} + \mathbf{F}_{k,hyst} + \mathbf{F}_{k,frict}\right) + \mathbf{C}_1 \frac{d}{dt}\mathbf{s}_1 + \mathbf{K}_1\mathbf{s}_1 = 0 \tag{22}$$

$$J_2 \frac{d^2}{dt^2}\theta_2 + D_2 \frac{d}{dt}\theta_2 + \hat{\mathbf{x}}_3 \cdot \sum_k \left[\mathbf{r}_{2,k} \times \left(\mathbf{F}_{k,elast} + \mathbf{F}_{k,hyst} + \mathbf{F}_{k,frict}\right)\right] + E_{2-3}\left(\frac{d}{dt}\theta_2 - \frac{d}{dt}\theta_3\right) + G_{2-3}(\theta_2 - \theta_3) = 0 \tag{23}$$

$$\mathbf{M}_2 \frac{d^2}{dt^2}\mathbf{s}_2 + \sum_k \left(\mathbf{F}_{k,elast} + \mathbf{F}_{k,hyst} + \mathbf{F}_{k,frict}\right) + \mathbf{C}_2 \frac{d}{dt}\mathbf{s}_2 + \mathbf{K}_2\mathbf{s}_2 = 0 \tag{24}$$

$$J_3 \frac{d^2}{dt^2}\theta_3 + D_3 \frac{d}{dt}\theta_3 - E_{2-3}\left(\frac{d}{dt}\theta_2 - \frac{d}{dt}\theta_3\right) - G_{2-3}(\theta_2 - \theta_3) - T_B = 0 \tag{25}$$

where:

$$\mathbf{s}_i = \begin{bmatrix} s_{i,1} & s_{i,2} & s_{i,3} \end{bmatrix}^T, \quad \mathbf{M}_i = \begin{bmatrix} M_{i,1} & & \\ & M_{i,2} & \\ & & M_{i,3} \end{bmatrix}, \quad \mathbf{C}_i = \begin{bmatrix} C_{i,1} & & \\ & C_{i,2} & \\ & & C_{i,3} \end{bmatrix}, \quad \mathbf{K}_i = \begin{bmatrix} K_{i,1} & & \\ & K_{i,2} & \\ & & K_{i,3} \end{bmatrix}, \; i=1,2$$

In essence, they resemble a typical system of dynamical equations for the rotor system (compacted in vector form) with the addition of the gear mesh force/ torque components. The exact tooth contact geometry and the resulting DOF coupling is represented implicitly in Eqs. (18-20), i.e. the stand-alone calculation of the contact force components.

Spur gears do not generate axial force components; therefore the components of the vector Eqs. (22, 24) along the x_3-axis are zero, so Eqs. (21-25) define a system of 7 2nd-order ordinary differential equations. The contact force components calculated from the gear meshing analysis render these equations non-linear, allowing the following phenomena to be simulated:

- tooth separation
- backlash
- dynamic centre-distance variations

The dynamical equations can be solved using standard time-domain numerical integration methods. Here a 4th order Runge-Kutta-Fehlberg method with 5th order convergence checking and intelligent step correction was used.

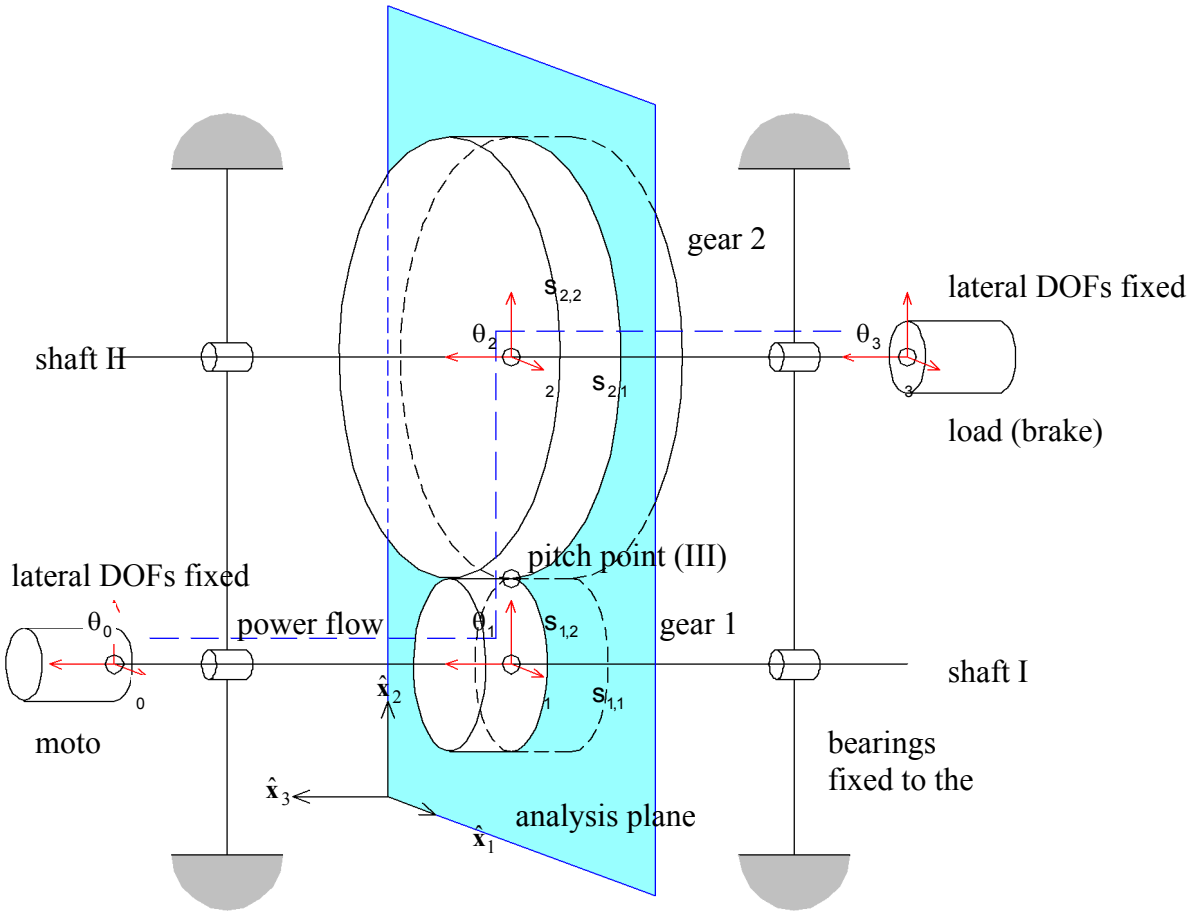

Fig. 2
Simulated single-stage gear speed reducer layout and DOF definition.

5. SIMULATION RESULTS

For the purpose of demonstrating the method a single stage gearbox layout was simulated with pressure angle of 20°, module of 2.5mm, tooth numbers of 25 (gear 1) and 50 (gear 2) respectively and gear width of 25mm. Centre distance was nominal at 93.75mm. All-steel gears and shafts were considered, with Young's modulus of 210GPa and Poisson's ratio of 0.3. Shaft diameters were respectively 30mm and 40mm and the length between bearings 50mm for both, in a symmetrical layout. Friction was simulated for a SAE 75W-90 lubricant.

Gear 1 is assumed errorless and indexing errors on gear 2 are assumed to follow a linear law, where the indexing error for each working surface j=1,2,...,N_2 is given by the formula:

$$\sigma^{(j)} = \sigma_o \frac{j-1}{N_2 - 1} \tag{26}$$

This is by far one of the most problematic distributions of indexing errors, as it produces a 'dropped tooth', which causes severe mesh excitation at the rotating shaft frequency and its harmonics [1]. To consider the combined effect of errors in both gears, σ_o can be set equal to the sum of the maximum indexing errors of both gears. This in fact gives a more pessimistic prediction than if the errors were considered separately, so the results can be considered to include a safety margin. The choice of concentrating indexing errors on gear 2 is made to minimise the number of independent parameters and allow for an easier visualisation and ultimately a more versatile method. Clearly, the employed TCA model can handle much more complicated distributions and combinations, if needed.

In the test cases employed in the following simulations various σ_o values and profile corrections are considered. Specialised in-house developed code was used to simulate the dynamic responses for the various test cases in the time domain, considering input speed = 100rad/s (954.9rpm) and output torque = 10 Nm. Both the torsional and the lateral vibration components are checked.
From the simulated vibration response the load factor is calculated as follows:

$$\text{load factor} = \frac{\text{maximum force}}{\text{nominal force}} \tag{27}$$

where the nominal force is calculated for static loading with nominal output torque.

6. SENSITIVITY ANALYSIS

The standard remedy for an anticipated maximum index error of σ_o would be to apply a profile modification of magnitude $m = \sigma_o$. In reality, the real indexing error σ_{or} will lie within a tolerance field $\sigma_{o}^{+U\sigma}_{-L\sigma}$ and the prescribed modification will also be implemented as m_r, which will lie within a tolerance field m^{+Um}_{-Lm}. Therefore:

$$\sigma_o - L\sigma \le \sigma_{or} \le \sigma_o + U\sigma, \quad m - Lm \le m_r \le m + Um \tag{28}$$

real maximum indexing error σ_{or}	actual modification m_r		
	$< \sigma_o$	$= \sigma_o$	$> \sigma_o$
$< m$	possible impact (1)	safe	safe, possible excessive vibration (3)
$= m$	impact (2) ←	nominal, marginally safe	safe
$> m$	impact (2)	impact (2)	possible impact (1)

(1) impact if real indexing error < real modification TE (2) insufficient modification (3) excessive modification

Table 1
Effect of different real indexing error and profile modifications on vibration excitation. ‘safe’ means no impact, but not necessarily low vibration

Obviously, any combination within those limits is to be expected in a set of manufactured gears, causing the dynamical response to fall anywhere within the load factor diagram. Possible combinations are summarised in Tab. 1. An immediate observation is that the $m = \sigma_o$ design is quite sensitive to tolerances, as it lies on the left-most edge of the ‘safe’ region; a small negative fluctuation of the actual modification will give rise to impacts, as is shown by the arrow in Tab. 1.

In conclusion, given the indexing error, an efficient and objective definition of the boundaries of the allowable load factor can be obtained by defining what increase of the load factor in relation to the optimal is considered acceptable. By plotting the simulated load factor results on a contour diagram the optimal design regions can be identified for the whole range of load factors.
The ‘sensitivity chart’ can be directly used as a nomogram to determine the acceptable and the optimal tolerance fields for the profile modification. Naturally, the width of the modification tolerance field is only a function of the employed modification process and is predetermined. So the calculated allowable limits will typically be used in determining the optimal nominal modification value (usually the middle of the tolerance field, Fig. 3).

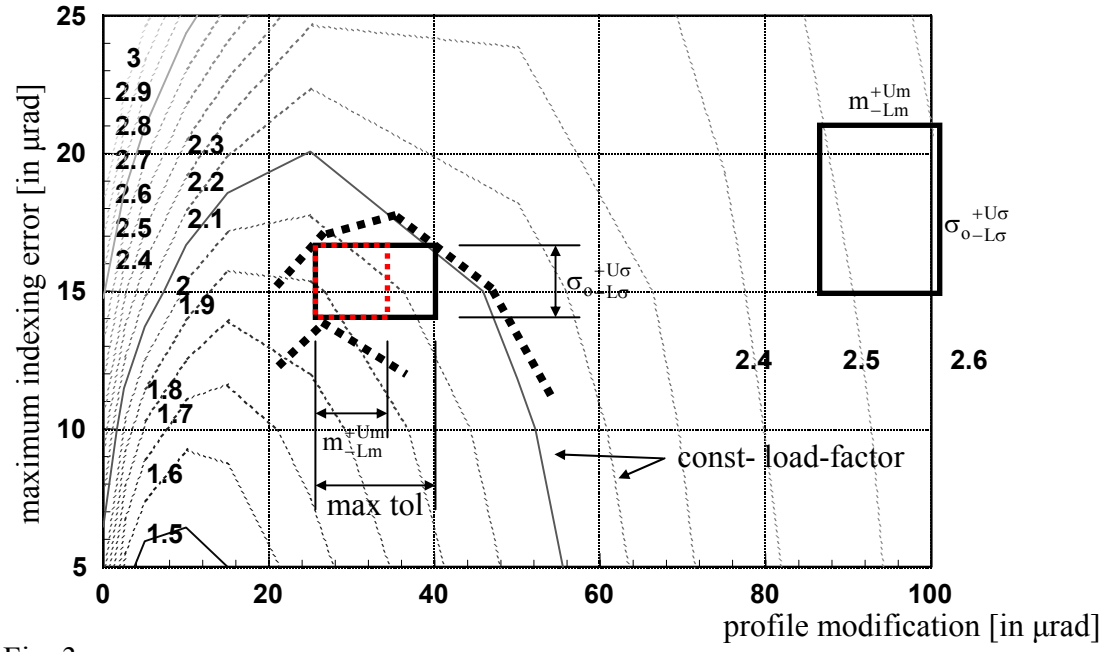

Fig. 3
Sensitivity chart

7. CONCLUSION

This paper addressed the uncertainty involved in estimating the real indexing error and in actually producing a prescribed modification that introduces tolerances in the design and manufacturing procedure, which are dependent on the accuracy of the measuring/ manufacturing equipment and even the practical feasibility of checking potentially large samples of batch-produced gears.
The exact geometry of tooth meshing was used as a starting point for a comprehensive dynamical modelling of gear systems, incorporating the effect of pitch errors, tooth separation, DOF coupling, and profile modifications producing a fundamentally non-linear model. Various possible combinations of error distributions and profile corrections were applied to the gear model, which was simulated dynamically to calculate the load factor. The results were presented in a sensitivity chart to allow for design choices such as to determine the acceptable and the optimal tolerance fields for the profile modification.

REFERENCES

[1] D. P. Townsend, *Dudley's Gear Handbook.* McGraw-Hill, New York, 1992
[2] Spitas V.A., Costopoulos T.N., Spitas C.A., Optimum gear tooth geometry for minimum fillet stress using BEM and experimental verification with photoelasticity, *Journal of Mechanical Design*, **128** (5), 2006, pp. 1159-1164.
[3] Spitas V., Spitas C., Numerical and experimental comparative study of strength-optimised AGMA and FZG spur gears, *Acta Mechanica*, **193** (1-2), 2007, pp. 113-126.
[4] Yeh T., Yang D., Tong S., Design of new tooth profiles for high-load capacity gears, *Mechanism and Machine Theory*, **36**, 2001, pp. 1105-1120
[5] Spitas C., Spitas V., A FEM study of the bending strength of circular fillet gear teeth compared to trochoidal fillets produced with enlarged cutter tip radius, *Mechanics Based Design of Structures and Machines*, **35** (1), 2007, pp. 59-73.
[6] Spitas C., Spitas V., Effect of cutter pressure angle on the undercutting risk and bending strength of 20° involute pinions cut with equivalent nonstandard cutters, *Mechanics Based Design of Structures and Machines*, **36** (2), 2008, pp. 189-211.
[7] Litvin F., L., Qiming L., Kapelvich A., L., Asymmetric modified spur gear drives reduction of noise, localization of contact, simulation of meshing and stress analysis, *Computer Methods in Applied Mechanics and Engineering*, **188**, 2000, pp. 363-390

[8] Kapelevich, A. L., Geometry and design of involute spur gears with asymmetric teeth, *Mechanism and Machine Theory*, **35**, 2000, pp. 117-130
[9] Spitas V., Spitas C., Costopoulos T., Reduction of tooth fillet stresses using novel one-sided involute asymmetric gear design, Mechanics Based Design of Structures and Machines, **37** (2), 2009, pp. 157-182
[10] Spitas V.A., Costopoulos T.N., Spitas C.A., Optimum gear tooth geometry for minimum fillet stress using BEM and experimental verification with photoelasticity, *Journal of Mechanical Design*, **128** (5), 2006, pp. 1159-1164.
[11] Spitas V., Spitas C., Four-parametric design study of the bending strength of circular-fillet versus trochoidal-fillet in gear tooth design using BEM, *Mechanics Based Design of Structures and Machines*, **35** (2), 2007, pp. 163-178.
[12] Ciavarella M., Demelio G., Numerical methods for the optimisation of specific sliding, stress concentration and fatigue life of gears, *International Journal of Fatigue*, **21**, 1999, pp. 465-474
[13] Spitas C., Spitas V., Generating standard 20° involute pinions with increased fillet strength by using 25° rack cutters with non-standard module, *Journal of Mechanical Engineering Science*, **220** (8), 2006, pp. 1297-1304.
[14] Spitas V., Spitas C., Optimizing involute gear design for maximum bending strength and equivalent pitting resistance, *Journal of Mechanical Engineering Science*, **221** (4), 2007, pp. 479-488
[15] R. G Munro, *Data item on profile and lead correction*, BGA Technical Publications, 1988
[16] AGMA 170.01, *Design guide for vehicle spur and helical gears*, AGMA, 1976
[17] AGMA 109.16, *Profile and longitudinal corrections on involute gears*, AGMA, 1965
[18] *Maag Taschenbuch*, Maag Zahnräder AG, Zürich, 1985
[19] D. W. Dudley, *Handbook of practical gear design*, McGraw-Hill, New York, 1984
[20] G. Niemann, H. Winter, *Maschinenelemente, Band II*, Springer Verlag, 1983
[21] F. L. Litvin, *Gear Geometry and Applied Theory*, Prentice-Hall, Englewood Cliffs, NJ, 1994
[22] I. H. Seol, D. H. Kim, The kinematic and dynamic analysis of crowned spur gear drive, *Computer Methods in Applied Mechanics and Engineering*, **167** pp. 109-118, 1998
[23] C. Spitas, V. Spitas, Calculation of overloads induced by indexing errors in spur gearboxes using multi-degree-of-freedom dynamical simulation, *Journal of Multi-Body Dynamics*, **220** (4), 2006, pp. 273-282
[24] Spitas C., Spitas V., Direct analytical solution of a modified form of the meshing equations in two dimensions for non-conjugate gear contact, *Applied Mathematical Modelling*, **32** (10), 2008, pp. 2162-2171.
[25] Spitas C., Costopoulos Th., Spitas V., Direct analytical solution of the inverse gear tooth contact analysis problem, *Inverse Problems in Science and Engineering*, **16** (2), 2008, pp. 171-186.
[26] Spitas C., A continuous piecewise internal friction model of hysteresis for use in dynamical simulations, *Journal of Sound and Vibration*, **324** (1-2), 2009, pp. 297-316.
[27] R. W. Cornell, Compliance and stress sensitivity of spur gear teeth, *Journal of Mechanical Design*, **103** pp. 447-459, 1981
[28] S. Timoshenko, J. Goodier, *Theory of Elasticity*, 3rd Ed., McGraw-Hill, New York, 1970
[29] R. Casuba, J. W. Evans, An extended model for determining dynamic loads in spur gearing, ASME *Journal of Mechanical Design*, **103** pp. 398-409, 1981
[30] N. E. Dowling, *Mechanical behavior of materials*, 2nd Ed., Prentice Hall, 1998.
[31] M.-H. Tsai, Y.- C. Tsai, A method for calculating static transmission errors of plastic spur gears using FEM evaluation, *Finite Elements in Analysis and Design*, **27**, 1997, pp. 345-357
[32] R. Muthukumar, M. R. Raghavan, Estimation of gear tooth deflection by the finite element method, *Mechanism and Machine Theory*, **22**, 1987, pp. 177-181
[33] A. Andersson, L. Vedmar, A dynamic model to determine vibrations in involute helical gears, *Journal of Sound and Vibration*, **206**, 2003, pp. 195-212